AD-A041 215 ALABAMA UNIV IN HUNTSVILLE F/G 20/5
NEW MATERIALS FOR CHEMICAL LASER WINDOWS.(U)
FEB 77 J A HARRINGTON , D A GREGORY N00014-76-C-0941
UNCLASSIFIED UAH-RR-198 NL

1 OF 1
ADA041215

END

DATE
FILMED
8-77

UAH Research Report No. 198

The University of Alabama in Huntsville

P. O. Box 1247
Huntsville, Alabama 35807

Final Report
Contract N00014-76-C-0941

By

James A. Harrington
Principal Investigator

Prepared for

Naval Research Laboratory
4555 Overlook Ave., S. W.
Washington, D. C. 20375

February 1977

to the intrinsic absorption in these hosts. In all cases, the measured absorption has been found to be greater than the intrinsic value. In addition to the absorption measurements on these substances, some recent optical absorption measurements on water repellent coatings on KCl will be discussed.

"Analysis of Laser Calorimetric Data"

Adiabatic laser calorimetry, which is the widely used method for studying the absorption coefficients of low-loss materials, can be adapted to study both the bulk and surface absorption by using a long rod sample geometry. In the limiting case of small heat losses, calculations of the thermal rise curves obtained in laser calorimetry indicate that two regions of constant slope can be expected. The first of these can be identified with the bulk absorption coefficient only and the second with the sum of the surface and bulk absorptions. Experimental data illustrating this two-slope behavior is presented.

"Surface and Bulk Absorption Measurements - Two Methods of Analysis"

Classical heat flow has been employed in a previous paper to determine bulk and surface absorption coefficients for long, highly transparent samples. Here we present a brief outline of this method and an older method which utilizes the slopes of the temperature-time curves directly to separate surface and bulk absorption. We then compare the results of the two methods and give possible sources of error along with suggestions as to when each method of analysis would be preferred.

SECURITY CLASSIFICATION OF THIS PAGE (When Data Entered)

REPORT DOCUMENTATION PAGE

READ INSTRUCTIONS BEFORE COMPLETING FORM

1. REPORT NUMBER: UAH-RR-198
2. GOVT ACCESSION NO.
3. RECIPIENT'S CATALOG NUMBER

4. TITLE (and Subtitle)
(No title - collection of papers)
See Block 20

5. TYPE OF REPORT & PERIOD COVERED
Final Report - June - Dec 76

6. PERFORMING ORG. REPORT NUMBER
UAH Research Report No. 198

7. AUTHOR(s)
James A. Harrington, Herbert B. Rosenstock*
Don A. Gregory, M. Hass*
*Naval Research Laboratory

8. CONTRACT OR GRANT NUMBER(s)
N00014-76-C-0941

9. PERFORMING ORGANIZATION NAME AND ADDRESS
The University of Alabama in Huntsville
P. O. Box 1247
Huntsville, AL 35807

10. PROGRAM ELEMENT, PROJECT, TASK AREA & WORK UNIT NUMBERS

11. CONTROLLING OFFICE NAME AND ADDRESS
Naval Research Laboratory
Washington, DC 20375

12. REPORT DATE
February 1977

13. NUMBER OF PAGES
53

14. MONITORING AGENCY NAME & ADDRESS(if different from Controlling Office)

15. SECURITY CLASS. (of this report)
UNCLASSIFIED

15a. DECLASSIFICATION/DOWNGRADING SCHEDULE

16. DISTRIBUTION STATEMENT (of this Report)

Approved for public release - distribution unlimited

17. DISTRIBUTION STATEMENT (of the abstract entered in Block 20, if different from Report)

18. SUPPLEMENTARY NOTES

19. KEY WORDS (Continue on reverse side if necessary and identify by block number)

Chemical lasers, laser windows, infrared materials, multiphonon absorption, optical absorption, water repellent coatings.

20. ABSTRACT (Continue on reverse side if necessary and identify by block number)

"New Materials for Chemical Laser Windows"

Many of the more common materials such as the alkaline earth fluorides, ZnSe, and the alkali halides have been studied for use as low loss windows on DF-HF chemical lasers yet there remain others which have received little or no attention at these wavelengths. We have begun to investigate some of these other materials in hopes of finding additional low absorbing materials which show potential as laser windows. Specifically, our measurements of the optical absorption in $LiYF_4$, Yttralox, ZnS, CdTe, KBr, SrF_2, and KRS-5 will be discussed and related

DD FORM 1 JAN 73 1473 EDITION OF 1 NOV 65 IS OBSOLETE
S/N 0102-LF-014-6601

SECURITY CLASSIFICATION OF THIS PAGE (When Data Entered)

UAH Research Report No. 198

The University of Alabama in Huntsville

P. O. Box 1247
Huntsville, Alabama 35807

Final Report
Contract N00014-76-C-0941

By

James A. Harrington
Principal Investigator

Prepared for

Naval Research Laboratory
4555 Overlook Ave., S. W.
Washington, D. C. 20375

February 1977

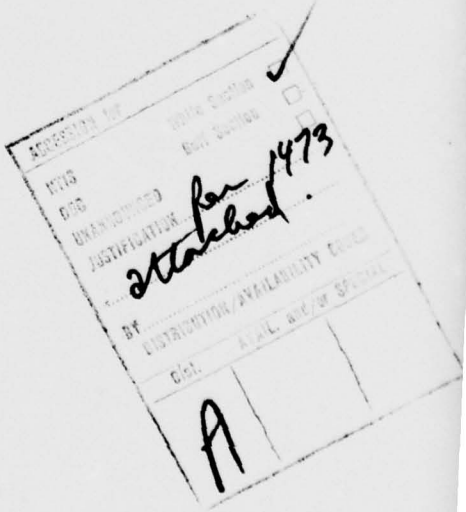

PREFACE

This report describes work on Low Loss Window Materials for chemical lasers under contract No. N00014-76-C-0941. This is a final report prepared for the Navel Research Laboratory, Washington, D. C. Participating in the research were, in addition to the principal investigator, James A. Harrington, Don A. Gregory, William Otto, Charles E. Patty, Jr. and Donald R. Hulsey.

TABLE OF CONTENTS

SUMMARY

The research into chemical laser window material has now turned to some degree into investigating other materials which have received little or no attention at the HF and DF laser wavelengths. Specifically, our measurements of the absorption in $LiYF_4$, Yttralox, ZnS, CdTe, KBr, SrF_2, and KRS-5 will be discussed and related to the intrinsic absorption in these hosts.

Further investigation into the long bar method of laser calorimetry is presented along with two methods of analyzing the temperature vs. time curve. Finally these two methods are compared using actual data obtained via the two methods of analysis.

NEW MATERIALS FOR CHEMICAL LASER WINDOWS*

James A. Harrington
Physics Department
University of Alabama in Huntsville
Huntsville, Alabama 35807

Many of the more common materials such as the alkaline earth fluorides, ZnSe, and the alkali halides have been studied for use as low loss windows on DF-HF chemical lasers yet there remain others which have received little or no attention at these wavelengths. We have begun to investigate some of these other materials in hopes of finding additional low absorbing materials which show potential as laser windows. Specifically, our measurements of the optical absorption in $LiYF_4$, Yttralox, ZnS, CdTe, KBr, SrF_2, and KRS-5 will be discussed and related to the intrinsic absorption in these hosts. In all cases, the measured absorption has been found to be greater than the intrinsic value. In addition to the absorption measurements on these substances, some recent optical absorption measurements on water repellent coatings on KCl will be discussed.

Key words: Chemical lasers; laser windows; infrared materials; multiphonon absorption; optical absorption; water repellent coatings.

1. Introduction

During the past several years, a wide variety of materials have been studied for use as low loss windows on high powered infrared lasers. At DF/HF chemical laser wavelengths, the range of potentially low loss materials is particularily wide and the optical absorption in the most common hosts such as the alkali halides, alkaline earth fluorides, ZnSe, Si, Ge, Al_2O_3, and MgO has been previously discussed [1,2][1]. There remain, however, other promising materials which have received little or no attention at these wavelengths. In this investigation, we report the results of our optical absorption measurements at DF and HF wavelengths on some less studied substances (Yttralox, KRS-5, ZnS, CdTe, and $LiYF_4$) as well as on some improved KBr and polycrystaline SrF_2. In addition to these measurements, the optical absorption in polymeric (water repellent) coatings on KCl will be presented.

2. Experimental Procedure and Techniques

The optical absorption was measured using standard laser calorimetric techniques [3]. In order to minimize surface contamination, all samples were measured in a vacuum calorimeter. In the case of SrF_2, a special vacuum calorimeter was used so that the samples could be baked out under vacuum and then measured without moving the samples (cf section 3.2). The cw DF/HF chemical laser used as a source was constructed from our own design and delivered from 5 to 10 watts of multiline power.

Samples were supplied for measurement from a variety of laboratories engaged in state-of-the-art materials preparation. Each sample was cleaned with spectrograde CCl_4 just prior to measurement. In instances when the surface quality looked particularly bad as viewed under a Nomarski microscope, the surfaces were mechanically polished, cleaned, and then remeasured. When this was done, the absorption was always less than the initial value. Examples of this behavior are noted in the next section.

3. Experimental Results

3.1 Semiconductors

Two semiconductors, which had previously not been measured, were studied. Single crystal CdTe obtained from II-VI, Inc. was found to have an absorption coefficient β at DF (3.8 μm) and HF (2.8 μm) wavelengths of:

CdTe β (DF) = 4.8×10^{-3} cm^{-1}

β (HF) = 5.3×10^{-3} cm^{-1}

These values are approximately an order of magnitude higher than the values reported by Deutsch [4] at CO_2 and CO wavelengths. A sample of CVD ZnS was obtained from Raytheon. In the past this has been a high loss material with a measured $\beta(CO_2)$=0.15 cm^{-1} [4]. At chemical laser wavelengths, however, we

*Work supported by DARPA and ONR.

[1]Figures in brackets indicate the literature references at the end of this paper.

measured smaller absorption as follows:

ZnS β (DF) = 0.049 cm^{-1}

β (HF) = 0.024 cm^{-1}

3.2 Raytheon Cast SrF_2

Three samples (VHP 597) of the most current, polycrystaline SrF_2 material were obtained from Raytheon. The three pieces enabled us to obtain β for four different lengths L ranging from 0.5 to 2 cm and thus to plot βL vs L for separation of bulk and surface absorption contributions from the total absorption.

The first measurements performed on the as-received samples are shown at 3.8 μm in figure 1. It can easily be seen from the figure that the absorption data (●) are quite scattered and therefore no reliable surface and bulk separation is possible. A similar result, not shown, was obtained at 2.7 μm. This scatter in the data is often due to unequal preparation or contamination of the sample surfaces. In order to minimize this problem, each sample was cleaned in trichloroethylene and then mounted in a special vacuum calorimeter for a bakeout at 200°C for several hours under vacuum. The samples were then cooled and β remeasured without breaking vacuum. These remeasured absorptions, which are plotted in figure 1 (▲), yield more consistent data and thus a least squares fit to the data was made. From the slope and intercept of this fit the following bulk (β_B) and surface (β_S) absorption coefficients are obtained:

$$\beta_B = 5.4 \times 10^{-5}\ cm^{-1}$$

$$\beta_S = 5.3 \times 10^{-5}/\text{surface}$$

The bulk value of $5.4 \times 10^{-5} cm^{-1}$ represents the smallest absorption of any sample measured to date at 3.8 μm. Unfortunately, the results after bakeout at 2.7 μm were again quite scattered and it was not possible to fit the data. A summary of all data for these samples is given below in table 1.

Table 1. Optical absorption in SrF_2 (Raytheon VHP 597)

Sample Condition	Wavelength	$\overline{\beta_T}(cm^{-1})$	$\beta_B(cm^{-1})$	β_S/surface
As-received	DF	1.6×10^{-4}	--	--
	HF	4.7×10^{-4}	--	--
Vacuum bakeout	DF	1.6×10^{-4}	5.4×10^{-5}	5.3×10^{-5}
	HF	4.1×10^{-4}	--	--

The total absorption coefficient $\overline{\beta_T}$ is the average β obtained from the three samples.

3.3 Alkali Halides

KRS-5 is an attractive substance for a laser window because of its resistance to environmental attack. It has received little attention, however, due to its relatively high loss at CO_2 frequencies [4]. At DF and HF wavelengths we have measured the following absorption in a sample of Harshaw KRS-5:

KRS-5 β (DF) = $2.3 \times 10^{-3}\ cm^{-1}$

β (HF) = $3.5 \times 10^{-3}\ cm^{-1}$

Recently grown single crystal KBr was obtained from Dr. Phil Klein of NRL for our absorption studies. This material was RAP processed [5] and represents some of the best KBr we have measured to date. Table 2 summarizes our absorption coefficient measurements on the samples as-received and

Table 2. Optical Absorption in KBr

Sample No.	Surfaces	β_T (DF) $[cm^{-1}]$	β_T (HF) $[cm^{-1}]$
B-324	As-received	3.6×10^{-4}	4.2×10^{-4}
	Mech. Polish	2.2×10^{-4}	3.2×10^{-4}
B-326	Mech. Polish	1.3×10^{-4}	4.1×10^{-4}

after a mechanical polish. It can be seen that polishing just prior to measurement lowers the ab-

sorption as might be expected for a hydroscopic material yet the absorption still remains well above the intrinsic value for KBr. Further surface treatment such as chemical etching should be done to try to minimize surface absorption.

3.4 Yttralox

Yttralox [Y_2O_3(90%): ThO_2(10%)] is an oxide with many attractive features as a potential low loss laser window. It has the usual strength and environmental resistance typical of oxides while at the same time exhibiting lower absorption than, for example, sapphire [1]. The Yttralox obtained for this study was supplied by General Electric [6].

The infrared absorption spectrum for Yttralox is shown in figure 2. An extrapolation of the multiphonon edge to $\beta_{int}(DF)=2.6\times10^{-5}cm^{-1}$ and $\beta_{int}(HF)=4.6\times10^{-9}cm^{-1}$ indicates the very low intrinsic values for this material at the chemical laser wavelengths. However, an extrinsic band is present in the as-received material. This band, unfortunately, appears directly between the DF and HF frequencies and is responsible for the higher absorption in this region.

In order to improve this material it is necessary to reduce the extrinsic absorption band centered near 3 μm. One method used to minimize this band is a reheating of the sample in a small amount ($\sim$10 ppm) of oxygen at high temperature ($\sim1700^{o}C$). In reheating the sample whose absorption is shown in figure 2, the extrinsic band completely disappeared. In this treatment, oxygen is presumably being forced into the Yttralox and the likely OH^- contaminant removed. On remeasuring β calorimetrically, the DF β in one sample (not shown in figure 2) decreased by a factor of 6 and the HF β by a factor of 4 [1].

It would seem that the most likely contaminant would be OH^- and that it is being at least partially removed in the retreatment process described above. Sulfur containing compounds, however, are also a possible source of contamination. In some cases the starting powder is ball-milled and in some cases this step is eliminated from the processing procedure. Ball-milling can introduce sulfur and, therefore, we have looked at different samples which are identical in processing except for the ball-milling operation. For those samples which involved the ball-milling operation, the absorption was always less at both DF and HF wavelengths than the corresponding samples which did not include ball-milling in their processing. Therefore, we cannot conclude that sulfur is definitely an impurity contributing to the extrinsic band near 3 μm.

3.5 Li YF_4

Li YF_4 is a potentially low loss material with good environmental resistance, a low index of refraction (1.46), and relatively high thermal conductivity ($0.044\ ^{W}/_{cm\ ^{o}K}$). The infrared absorption of undoped, single crystal Li YF_4 obtained from Sanders Assoc., Inc. is shown in figure 3. Included on the figure are our calorimetrically measured absorption coefficients

$$\text{Li } YF_4 \qquad \beta\ (DF) = 6.3\times10^{-3}\ cm^{-1}$$
$$\beta\ (HF) = 4.1\times10^{-3}cm^{-1}$$

along with the much smaller extrapolated intrinsic values. Again it can be seen that the measured absorptions lie well above the multiphonon edge indicating that the absorption is extrinsically limited.

3.6 Polymeric coatings

Water-repellent coatings have been produced to protect hydroscopic materials such as KCl. These coatings have, as well, to be evaluated in terms of optical absorption. To study the DF and HF absorption, Research Triangle deposited a water repellent, polymer coating on one-half of a KCL substrate. Our absorption measurements on this half-coated substrate are given in table 3. Unfortunately, the

Table 3. Polymeric coatings on KCl

Sample Section	$\beta_T(DF)\ [cm^{-1}]$	$\beta_T(HF)\ [cm^{-1}]$
Uncoated	1.9×10^{-3}	1.3×10^{-2}
Coated	2.1×10^{-3}	1.6×10^{-2}

total absorption in the uncoated half is essentially the same as the coated half, within experimental

error, so that it is impossible to extract from the data the absorption in the polymeric coating alone. All that can be said is that the coating material may have a low absorption but reliable coating absorptions cannot be obtained until better KCl substrate material is used.

4. Conclusions

The optical absorption in all of the materials studied has been found to be extrinsically limited. In the case of some materials such as Yttralox, the extrinsic bands are visible and methods have been attempted to reduce these bands near 3 μm. Yttralox, as well as, $LiYF_4$, and CdTe are previously little studied materials which could be improved through further materials processing. This would be especially profitable for Yttralox and $Li\ YF_4$ since they have appealing physical properties. Other materials such as ZnS and KRS-5 have absorption coefficients too high to be viable alternatives for low loss windows.

5. Acknowledgments

The author gratefully acknowledges the assistance of D.A. Gregory and W. Otto, Jr. for technical assistance in these measurements.

6. References

[1] Harrington, J.A., Gregory, D.A., and Otto, W.F., Appl. Optics, Aug., 1976 (to be published).

[2] Harrington, J.A., Gregory, D.A., and Otto, W.F., Fifth Conference on Infrared Laser Window Materials, Las Vegas, NV, 1975, p. B71.

[3] Hass, M., Davisson, J.W., Klein, P.H., and Boyer, L.L., J. Appl. Phys. 45, 3959 (1974).

[4] Deutsch, T.F., J. of Elect. Mat. 4, 663 (1975).

[5] Klein, P.H., Fifth Conference on Infrared Laser Window Materials, Las Vegas, NV, 1975, p. 983.

[6] Greskovich, C. and Woods, K.N., Amer. Cer. Soc. Bull. 52, 473 (1973).

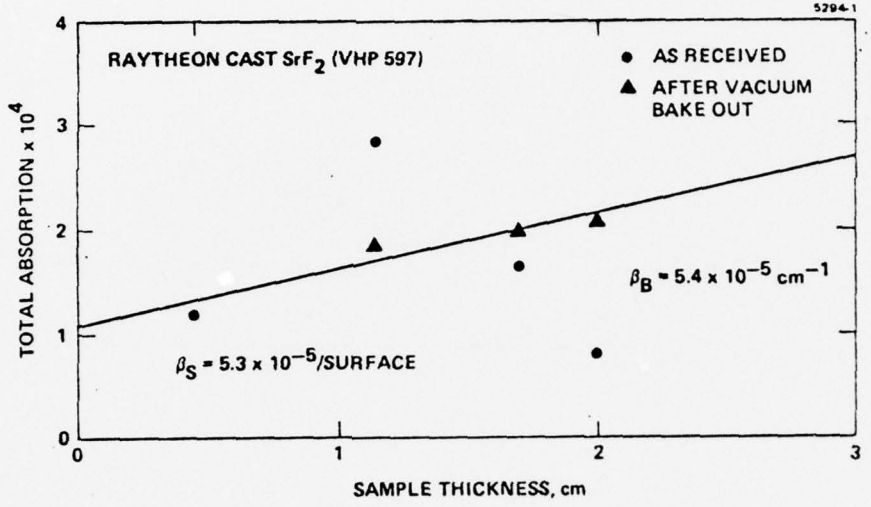
5294-1
RAYTHEON CAST SrF_2 (VHP 597)
AS RECEIVED
AFTER VACUUM BAKE OUT
$\beta_B = 5.4 \times 10^{-5}$ cm^{-1}
$\beta_S = 5.3 \times 10^{-5}$/SURFACE
TOTAL ABSORPTION x 10^4
SAMPLE THICKNESS, cm
0
1
2
3
4

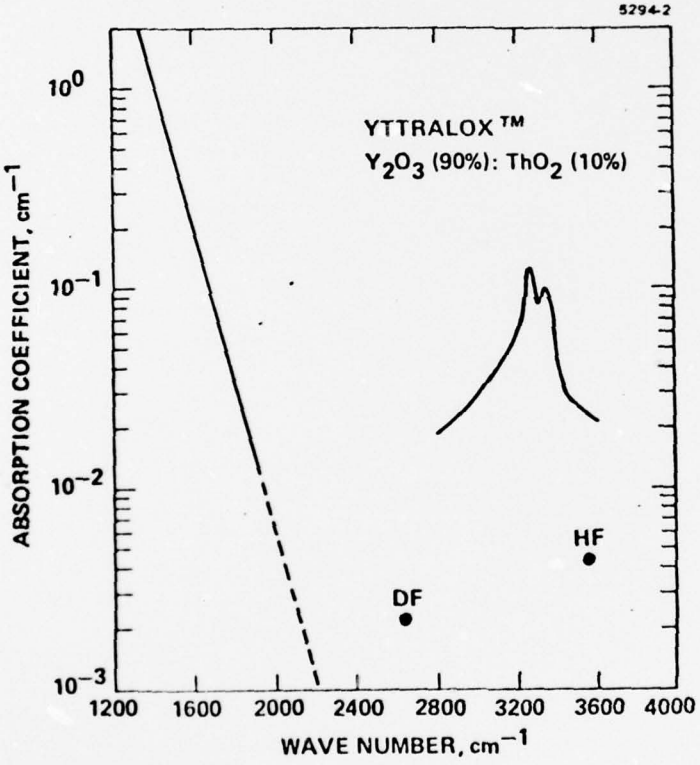
5294-2
YTTRALOX ™
Y_2O_3 (90%): ThO_2 (10%)
HF
DF
ABSORPTION COEFFICIENT, cm^{-1}
10^0
10^{-1}
10^{-2}
10^{-3}
1200
1600
2000
2400
2800
3200
3600
4000
WAVE NUMBER, cm^{-1}

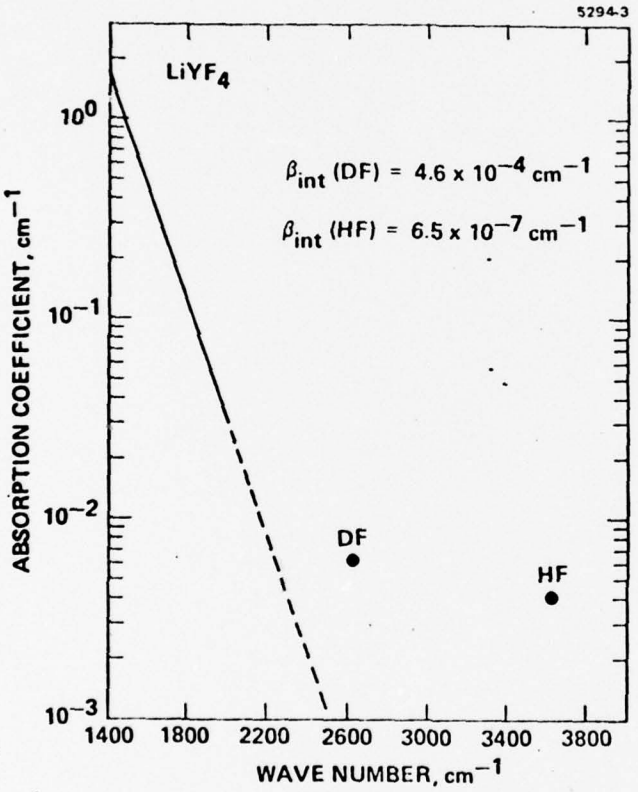
5294-3
LiYF4
β_{int} (DF) = 4.6 x 10^{-4} cm^{-1}
β_{int} (HF) = 6.5 x 10^{-7} cm^{-1}
DF
HF
ABSORPTION COEFFICIENT, cm^{-1}
10^{0}
10^{-1}
10^{-2}
10^{-3}
1400
1800
2200
2600
3000
3400
3800
WAVE NUMBER, cm^{-1}

7. Figure captions

Figure 1. Intrinsic absorption in Raytheon cast Sr F_2 at DF laser frequencies.

Figure 2. Infrared absorption in Yttralox. Note the extrinsic band near 3 μm and the extrinsically limited DF and HF absorption coefficients.

Figure 3. Infrared absorption in Li YF_4.

ANALYSIS OF LASER CALORIMETRIC DATA*

H.B. Rosenstock and M. Hass
Naval Research Laboratory
Washington, D.C. 20375

D.A. Gregory and J.A. Harrington
University of Alabama in Huntsville
Huntsville, Alabama 35807

ABSTRACT

Adiabatic laser calorimetry, which is the widely used method for studying the absorption coefficients of low-loss materials, can be adapted to study both the bulk and surface absorption by using a long rod sample geometry. In the limiting case of small heat losses, calculations of the thermal rise curves obtained in laser calorimetry indicate that two regions of constant slope can be expected. The first of these can be identified with the bulk absorption coefficient only and the second with the sum of the surface and bulk absorptions. Experimental data illustrating this two-slope behavior is presented.

I. INTRODUCTION

One of the more difficult problems in measuring the absorption coefficients of low-loss materials has been the separation of surface and bulk effects.[1,2] A way of establishing the magnitude of bulk absorption even in the presence of much larger surface absorption was indicated in previous work from this laboratory using a modification of the widely used technique of laser calorimetry.[3,4] Here, it was shown that by use of long rod sample geometries with axial heating, a separation between surface and bulk absorption could be achieved by analyzing the time dependence of the thermal rise curves. For short times, it could be shown that the thermal rise curves depended only upon the bulk absorption and did not depend upon the surface contribution. In subsequent work,[5] it was shown that the surface absorption contribution, as well as the bulk, could be evaluated by a detailed study of the complete thermal rise curve of a long rod sample in which explicit knowledge of the thermal diffusivity is required.

In this present work, a simple approximation method for evaluating surface absorption is presented and justified. This method is useful in establishing whether significant surface absorption is present and its approximate magnitude. The method is based upon considerations of the three-dimensional heat equation and is illustrated by calculations and experimental data. Basically, it is shown that the thermal rise curves of axially heated samples under certain conditions consists of two regions of constant slope, the first of which can be identified with

the bulk absorption noted previously and the second with the total (surface + bulk) absorption. An accurate knowledge of the thermal diffusivity is not required and heat losses are readily incorporated into the analysis.

II. GENERAL ASPECTS

Laser calorimetry as a means of obtaining the low loss absorption coefficients of materials has been discussed in several reviews[1,2] and will not be dealt with here except for a few special remarks. Briefly, in adiabatic laser calorimetry, a sample is allowed to come to thermal equilibrium with its surroundings inside a blackened enclosure. After time t=0, the sample is irradiated by a cw laser beam. Absorption of radiation by the sample results in heating which is measured experimentally. In the limiting case of small heat losses and small samples, the detailed space-dependence of the temperature is ignored entirely. The temperature as measured by a thermocouple will increase linearly with time (after a few seconds to achieve thermalization) and is given by

$$mc\,(dT/dt) = AP \qquad (1)$$

where m is the sample mass, c is its specific heat, P is the power incident on the sample (for simplicity reflection losses are not considered here) and A the fraction that is absorbed (by either bulk or surface). Here the right hand side is just the total heat absorbed, and dT/dt on the left the temperature increase caused by it. Eq. (1) is appealing in its simplicity, but of limited usefulness. It can, for example, give no information on the details of the absorption processes lumped into the constant A.

A separation between bulk and surface absorption can be achieved by use of a long rod geometry with axial illumination and with the temperature sensor located on the periphery of the rod near the midpoint. In this case the time required for the heat absorbed by the end surface to reach the temperature sensor is longer than for the bulk which is axially heated. As a first approximation, consider an infinite medium of thermal diffusivity α and dimensionality D in which heat is turned on at time t=0. The temperature at a distance r from source reaches its maximum rate of increase at time $t=r^2/2\alpha D$, as shown in Appendix 2. Consider for example a KCl rod one cm in diameter and 10 cm long. Then this characteristic time will be about one sec for bulk absorption along the axis to reach the temperature sensor ($r=\frac{1}{2}$cm, D=2), but about 200 sec for heat generated at the end surface (r=5 cm, D=1.) Thus thermal rise data taken in a time range of about 1-200 sec would be expected to be representative of bulk absorption, while that taken for times longer than 200 sec would have a surface contribution as well.

These results are illustrated in Fig. 1 which shows a thermal rise curve calculated for a typical sample using the full solution of the three-dimensional heat equation.[7] The first constant slope can be identified with bulk absorption and after about 200 sec another constant slope appears which can be identified with the total (surface plus bulk) absorption. This identification can be expressed in a more quantitative form by considering the solution of the three-dimensional heat equation for a finite cylinder with vanishing heat losses, which is ob-

tained in Appendix I. In that case, the temperature T at the middle of the peripheral surface of the rod is, according to Eqs.(A10), (A13), (A16) and (A20)

$$T - T_s = \frac{P}{mc}\left\{\beta L\left(t - \frac{b^2}{8\alpha}\right) + 2S\left[t - \frac{b^2}{4\alpha} - \frac{\left(\frac{1}{2}L\right)^2}{6\alpha}\right]\right\} \qquad (2)$$

+ bulk transient terms + end surface transient terms, as shown in the Appendix. Here T_s is the temperature of the surroundings, β the bulk absorption coefficient per unit length, S the fraction absorbed at one end surface, t the time, and L, b, m, c, ρ, k, respectively the length, radius, mass, specific heat, density and conductivity of the sample and $\alpha = k/c\rho$. As it stands, Eq. (2) is valid for large t; at times before the heat from the surface arrives, the term involving S is to be omitted. The transient terms produce the smooth transition between regions of constant slope in the thermal rise curves and are neglected here. The factor, $r^2/8\alpha$, which is approximately the characteristic time for heat to travel from the axis to the periphery may also be neglected for our narrow rods, as $b \ll L$. Thus Eq. (2) can be simplified to

$$T - T_s = \frac{P}{mc}\begin{cases} \beta Lt & \text{short times} \\ \beta Lt + 2S\left[t - \dfrac{\left(\frac{1}{2}L\right)^2}{6\alpha}\right] & \text{long times} \end{cases} \qquad (3)$$

This confirms the calculated thermal rise curve of Fig. 1. The constant slope due to bulk absorption appears first; the surface contribution gives a larger total slope but manifests itself later. This can be more clearly seen by rearranging the long time expression in Eq. (3) giving

$$T - T_s = \frac{P}{mc} (\beta L + 2s) \left[t - \frac{2S}{\beta L + 2S} \frac{(\frac{1}{2}L)^2}{6\alpha} \right] \qquad (4)$$

Thus the slope in the long time region is proportional to the total absorption, $\beta L + 2S$, and the intercept depends upon the ratio of the surface to the total absorption.

For equal bulk and surface absorption as in the case calculated in Fig. 1, this intercept will be about 40 sec. At least where heat losses are very small, the magnitude of both the bulk and surface absorption can be established in a simple and straightforward way. The inclusion of heat losses adds additional complications because of a nonuniform temperature profile of the rod. But it will be seen shortly that this can be dealt with in a simple way for typical cases.

In order to gain some idea of the nature of thermal rise curves for various ratios of surface to bulk absorption, a number of calculations were carried out using the full solution of the heat equation[7] and are shown in Fig. 2. It can be seen that as expected the second slope appears somewhat earlier as the surface absorption increases. In order to obtain an idea of the thermal rise curves as a function of length, a number of calculations were carried out and are shown in Fig. 3. These results show that while long cylinders are obviously desirable, it is possible to employ shorter samples.

So far heat losses have been ignored. They are, however, difficult to eliminate in actual measurements, and have been

included in a previous calculation of the temperature distribution.[5] These involve a detailed comparison of experiment and theory. Most investigators have chosen to account for heat losses in a simple manner by use of a "sum-of-slopes" (sum of rising and falling slopes at a constant temperature) or the "three-slope" formula[8] which is more general. The latter two approaches assume instant thermalization in which the heat absorbed is presumed to be immediately dispersed through the sample. This is a reasonable approach for bulk absorption alone, or for the total absorption provided samples are small or approximately cubic or spherical shape, but not for either long rods with end surface absorption or for discs. Nevertheless, the "sum-of-slopes" or "three-slope" expressions do provide a convenient way of accounting for heat losses. Consequently, a calculation has been carried out and the exact result for surface only absorption has been compared with the "sum-of-slopes" formula. The calculations are illustrated in Fig. 4 for the case of no heat losses and where arbitrary heat losses have been included. The thermal rise slope for no heat losses has been compared with the "sum-of-slopes" where heat losses have been introduced. Note that an error less than 15% results. Thus, it is felt that for samples of about this size and thermal diffusivity, no appreciable error will result from use of the "sum-of-slopes" or three slope formulas.

III. EXPERIMENTAL RESULTS

A typical experimental situation is shown in Fig. 5 for KCl at 10.6 μm. For this sample, a two slope region behavior with

small heat losses is evident. The surface absorption is about equal to the bulk absorption. The time axis intercept is very close to $\frac{1}{2}(\frac{1}{2}L)^2/6\alpha$ = 25 sec expected from Eq. (4) is when the small jump at t=0 (due to scattering) when the laser is turned on is eliminated. After the laser is turned off the temperature continues rising (again ignoring the small jump due to scattering) because previously absorbed heat is still flowing to the thermocouple. After thermalization has been achieved in a time two or three times larger than $(\frac{1}{2}L)^2/6\alpha \sim 50$ sec, the temperature decreases slowly due to heat losses. For samples of this nature, the two slope behavior is readily observed. For crystals such as ZnSe, the process is more difficult to observe due to the higher thermal diffusivity which makes the characteristic time $(\frac{1}{2}L)^2/6\alpha$ comparable to the response time of the system for samples of a few cm length. For other samples such as silicate glasses, heat losses are greater and are not well fitted by simple "sum-of-slopes" or "three-slope" formulas.

A few additional comments about experimental techniques are in order, although most of this has been presented previously.[3,4] It should be stressed that time constants of the measuring system must be short compared to $r^2/6\alpha$ to make the above analysis valid. Fast time constants can be achieved by cementing the thermocouple to an aluminized spot on the sample. Use of an aluminized spot has been known to work well in reducing scattered light effects by reflection.[3] In much laser calorimetric work on infrared materials, the thermocouple is pressed into the sample using a plastic rod. This procedure increases the time

constant because of the high thermal mass of the rod. In addition, the sample is mounted on threads to reduce thermal linkage to the specimen holder. Some investigators have chosen to use vacuum calorimeters both to reduce heat losses and to remove surface absorbing films. This will help in reducing heat losses, but involves extra complexity.

In addition, we have also achieved better results when small laser spots are employed. Consequently, the output mode pattern of the laser should be checked.

Our principal conclusion and both the surface and bulk absorption can be established quite well using adiabatic laser calorimetry by using a long rod sample geometry.

FIGURE CAPTIONS

Fig. 1. Calculated thermal rise curve for a long rod of KCl having both surface and bulk absorption. Note a change in slope at about 80 sec. The time axis intercept is indicated by an arrow.

Fig. 2. Calculated thermal rise curves for a long rod of KCl having different amounts of surface absorption.

Fig. 3. Calculation thermal rise curves for long rods of KCl of different lengths but the same bulk absorption coefficient and same surface absorption.

Fig. 4. Calculated thermal rise curves for a long rod of KCl having only surface absorption. The cases of no heat losses and a large arbitrary heat loss are considered.

Fig. 5. Experimental thermal rise curve for KCl. Note a two slope behavior with approximately equal contributions to the heat from surface and bulk effects. The characteristic time $(\frac{1}{2} L)^2/6\alpha$ is about 50 sec for this sample. A small jump occurs on laser turnon and turnoff due to scattered light. The bulk absorption coefficient in this sample is 9×10^{-5} cm^{-1} and the surface absorption is 1.1 times the bulk absorption.

REFERENCES

*Supported in part by ONR Material Sciences Division

1. L.H. Skolnik, "A Review of Techniques for Measuring Small Optical Losses in Infrared Transmitting Materials", in Optical Properties of Highly Transparent Solids, edited by S.S. Mitra and B. Bendow (Plenum, New York, 1975), p. 405-434.
2. A. Hordvik, "Recent Advances in Measurement Techniques for Small Absorption Coefficients", Applied Optics 16, 000 (1976).
3. M. Hass, J.W. Davisson, H.B. Rosenstock, and J. Babiskin, "Measurement of Low Absorption Coefficients by Laser Calorimetry", Applied Optics 14, 1128-1130 (1975).
4. M. Hass, J.W. Davission, H.B. Rosenstock, J.A. Slinkman, and J. Babiskin, "Improved Laser Calorimetric Techniques", in Optical Properties of Highly Transparent Solids, edited by S.S. Mitra and B. Bendow (Plenum, New York, 1975) p. 435-442.
5. H.B. Rosenstock, D.A. Gregory, and J.A. Harrington, "Infrared Bulk and Surface Absorption of Nearly Transparent Crystals", Applied Optics 15, 2075-2079.
6. H.S. Carslaw and J.C. Jaeger, Conduction of Heat in Solids (Oxford U.P., 2nd edition, London, 1959 page 50.
7. H.B. Rosenstock in"High Energy Laser Windows" (Semi-Annual report No. 6, 30 September 1975, ARPA Order No. 2031, Naval Research Laboratory, Washington, D.C. 20375, page 15.
8. M. Hass, J.W. Davisson, P.H. Klein, and L.L. Boyer, "Infrared Absorption in Low-Loss KCl Single Crystals Near 10.6 μm", J. Appl. Phys. 45, 3959-3964 (1974).

9. E. Jahnke and F. Emde, "Tables of Functions" 4th edition (Dover, New York, 1945) page 143.

10. L.B. Jolley, "Summation of Series" 2nd edition (Dover, New York, 1961).

Formula (573) reads $\sum_{1}^{\infty}\cos 2n\pi\theta/(2n\pi)^2=[\theta^2-\theta-(1/6)]/4$

Formula (559) reads $2a^2\sum_{1}^{\infty}\cos n\theta/(n^2+a^2)=-1+\frac{a\pi\cosh a(\pi-\theta)}{\sinh a\pi}$

APPENDIX I - Temperature Distribution in an Insulated Cylinder

We have recently obtained[8] the following solution to the temperature distribution in a cylinder that is heated by a laser beam along the axis and looses heat at every surface:

$$T(r,z,t) = (2\pi P/k) \sum_{mn}\sum [R_n^2 Z_m^2/\gamma_{mn} J_o^2(\epsilon_n b)] \cdot \cdot u(\epsilon_m,z) J_o(\epsilon_n r)(\beta P_{1m}+SP_{2m}) \cdot \cdot [1-\exp(-\gamma_{mn}\alpha t)] \quad . \tag{A1}$$

Here r and z are the usual cylindrical coordinates, r=b, z=0 and z=L are the bounding surfaces, t is the time, T the temperature, $\alpha = k/c\rho$ is the thermal diffusivity, k is the thermal conductivity, c the specific heat and ρ the density of the sample, P the power of the laser beam, ß the bulk absorption coefficient (i.e. the fraction of P absorbed per unit distance traversed) and S the fraction of P absorbed by one end surface. R_n and Z_n are given by

$$R_n^{-2} = 2\pi^2 b^2[(H/\epsilon_n)^2 + 1]$$
$$Z_m^{-2} = H + (L/2)[\epsilon_m^2 + H^2] \tag{A2}$$

with H=h/k and h the coefficient of heat transfer at a boundary. u is given by

$$u(\epsilon_m,z) = \epsilon_m \cos\epsilon_m z + H\sin\epsilon_m z \quad , \tag{A3}$$

J_o is the Bessel function of order zero and the eigenvalues ϵ_m and ϵ_n are, respectively, the solutions of the transcendental equations

$$\tan \epsilon_m L = 2H\,\epsilon_m/(\epsilon_m^2 - H^2)$$
$$H\,J_o(\epsilon_n b) = \epsilon_n J_1(\epsilon_n b) \tag{A4}.$$

Finally

$$\epsilon_m P_{1m} = H(1-\cos\epsilon_m L) + \epsilon_m \sin\epsilon_m L \quad , \tag{A5}$$
$$P_{2m} = \epsilon_m \quad .$$

The reader may be able to verify that this indeed satisfies the heat equation

$$\nabla^2 T + \frac{g(z,r,t)}{k} = \frac{1}{\alpha}\frac{\partial T}{\partial t} \tag{A6}$$

with a source function

$$g = P\delta(r)(2\pi r)^{-1}\,[\beta + S\delta(z)] \tag{A7}$$

turned on at t=0 and general boundary conditions of the third kind

$$k\ \partial T/\partial n + hT = 0 \tag{A8}$$

(where n is the surface normal) at each of three boundary surfaces and reduces to T=0, the temperature of the surroundings, at t=0.

When surface absorption takes place at the surface z=L as well as at z=0, there are two ways of constructing the appropriate solution from (A1): Either replace $\delta(z)$ in (A7) by $[\delta(t)+\delta(z-L)]$, which has the consequence of replacing P_{2m} in (A5) by

$$P_{2m} = \epsilon_m(1 + \cos\epsilon_m L) + H \sin\epsilon_m L \quad ;$$

that is how is was done in Ref. 8. Alternatively, we can break (A1) up into two terms, writing it as $T=\beta T_1 + ST_2$ (when both T_1 and T_2 are double sums) and then replacing $u(\epsilon_m,z)$ by $[u/\epsilon_m,z) + u(\epsilon_m,L-z)]$ in T_2 only. That is the way we shall proceed below, after Eq. (A12).

Our purpose in this Appendix is to examine how all this simplifies if the sample is thermally insulated (no heat flow at the surface, h=0 in (A8) and elsewhere). First of all, we see from (A4) that

$$\epsilon_m = m\pi/L \quad , \quad m=0,1,2,... \tag{A9}$$

so that from (A3)

$$u(\epsilon_m, z) = \epsilon_m \cos \epsilon_m z;$$

similarly, the ϵ_n are now determined by $J_1(\epsilon_n b) = 0$, so that, for n=0, we get $\epsilon_o = 0$ and for $n > 0$, ϵ_n is nearly $\pi(n+\frac{1}{4})/b$ (though not exactly[9]). P_2 is given by (A5), and (A2) changes accordingly. The result is

$$T(r,z,t) = (P/VK)\{\beta LF(r,t) + S[F(r,t) + 2\,G(z,r,t)]\} \tag{A10}$$

where

$$F(r,t) = \alpha t + \sum_{n=1} \frac{J_o(\epsilon_n r)}{\epsilon_n^2 J_o^2(\epsilon_n b)} [1-e^{-\alpha \epsilon_n^2 t}] \tag{A11}$$

$$G(z,r,t) = \sum_{m=1} \cos \epsilon_m z \sum_{n=0} \frac{J_o(\epsilon_m r)}{(\epsilon_m^2+\epsilon_m^2)J_o^2(\epsilon_n b)} [1-e^{-\alpha (\epsilon_m^2+\epsilon_m^2)t}] \tag{A12}$$

Note that the coefficient of ß is now independent of z. Physically, this is a consequence of symmetry: if bulk heating is uniform along the axis, and the boundary conditions forbid flow across the end surfaces, then flow can proceed in the radial direction only.

The solution above, (A10) - (A12), applies to the source function (A7) - i.e. surface absorption at z=0 only. If the

surface at z=L absorbs equally, the coefficient of S in (A10) is to be replaced by $2F(r,t) + 2[G(z,r,t) + G(L-z,r,t)]$.

We observe that for large enough t, all the exponentials will vanish. In that case, the sums in F and G can be carried out for any point on the peripheral surface, r=b. For F this can be done directly and leads to

$$F(b,\infty) = \alpha t - b^2/8 \tag{A13}$$

For G, we interchange the order of the two summations,

$$G(z,b,\infty) = \sum_{n=0} H_n(z)/J_o(\epsilon_n b) \tag{A14}$$

where

$$H_n(z) = \sum_{m=1} \cos(m\pi z/L)/[(m\pi/L)^2 + \epsilon_n^2] \tag{A15}$$

H_o (for which $\epsilon_n = 0$) can be evaluated using formula (573) of Jolley's book[10] while all others yield to formula (559). The result can be written as

$$G(z,b,\infty) = -\frac{b^2}{16} + \frac{L^2}{12}(3\bar{z}^2 - 6\bar{z} + 2) + \frac{bL}{2}\sum_{n=1} B_n(\bar{z}) \tag{A16}$$

where

$$\bar{z} = z/L \tag{A17}$$

$$B_n(\bar{z}) = \frac{e^{-p_n\bar{z}}}{x_n J_o(x_n)} \quad \frac{1+e^{-2p_n(1-\bar{z})}}{1-e^{-2p_n}} \tag{A18}$$

$$p_n = Lx_n/b \tag{A19}$$

and the X_n the positive roots of $J_1(x)=0$. The x_n are approximately equal[9] to $(n+\frac{1}{4})\pi$ and, on account of the exponential $\exp(-p_n\bar{z})$, the sum over the x_n can be neglected unless $p_1\bar{z} < 3$ or $z < 3b/\pi \sim b$; that is, for all z except close to the end at which surface absorption takes place. For surface absorption by both ends we need, as noted above, the quantity $G(z,b,\infty) + G(L-z,b,\infty)$; this turns out to be

$$G(z,b,\infty) + b(L-z,b,\infty) = -\frac{b^2}{8} + \frac{L^2}{2}\left[\bar{z}(1-\bar{z})+\frac{1}{6}\right]+\frac{bL}{2}\sum_{n=1}[B_n(\bar{z})+B_n(1-\bar{z})] \quad (A20)$$

where, as before, the last sum may be neglected except for z within a distance of b from either end.

APPENDIX II - Arrival Times

In Appendix I, we have a correct but complicated solution to the heat flow problem we are interested in. In this Appendix, we present a much simpler solution which, though only approximately correct, will be useful in the more qualitative discussions of the paper proper. The simplification results from assuming a solid of infinite extent, that is to say, from ignoring the boundary conditions.

The homogeneous heat equation in D dimensions is

$$\nabla_D^2 T = \partial T/\alpha\partial t \quad . \quad (A21)$$

In a infinite solid, it has a solution

$$T = f(r_D,t) = (\pi\tau)^{-D/2} \exp(-r_D^2/\tau) \quad (A22)$$

where

$$\tau = 4\alpha t \quad (A23)$$

as is well known[6] and easily verified. Here the D-dimensional distance is given by $r_D^2=\sum_1^D r_i^2$ and the D-dimensional Laplacian is given by $\nabla_D^2=\sum_1^D \partial^2/\partial x_i^2$. Allowing our space to be D-dimensional rather than setting D=3 at the outset adds no serious complications and will be useful at the end of this Appendix.

Viewed as a function of r for fixed t, the solution T=f is seen to be a normalized Gaussian of width 4α t, and at t=0 in particular, it is an infinitely sharp Gaussian. For that reason, $f(r_D,t)$ is often referred to as the "source" solution

of the heat equation, as it describes the temperature at later times when an infinitely sharp source is inserted at the origin at time t=0. If, on the other hand, we look at it as a function of t for fixed r, we see that it starts at 0, remains small for a while, increases and reaches a peak, and then decays, reaching 0 again eventually.

In this paper, we are not interested in an infinitely sharp pulse inserted at t=0, but in a source at the origin which is turned on at t=0 and left on. The appropriate solution can be constructed from the "source" solution above by writing

$$F(r_D,t) = \int_o^t f(r_D,t-t')dt' = \int_o^t dsf(r_D,S) \qquad (A24)$$

Viewed as a function of t for fixed r , this new solution F starts from 0, increases, but does not reach a maximum at any finite time, but, rather, flattens out and approaches a constant temperature as t becomes large.

Now what we mean by "arrival time" at a point r from the origin is, of course, somewhat arbitrary. But a reasonable criterion might be the time at which F has its maximum slope as a function of t, that is, the time at which $0=\partial F/\partial t = \partial^2 f/\partial t^2$. Carrying out the double differentiation and solving for t, we obtain for the arrival time

$$t_A = r_D^2/2\alpha D \quad . \qquad (A25)$$

In the body of this paper, we usually consider a solid in the shape of a long, thin cylinder which is heated in two different ways: by "bulk absorption" - that is to say, by a heat source along the axis of the cylinder - and by "surface absorption" -

that is to say, by a heat source at one of the end surfaces. In both cases, the temperature is usually measured at the mid-point on the peripheral surface of the cylinder, far away from either end. It follows that in the first case, the heat flow will be in a radial direction, that is to say essentially 2-dimensional, whereas in the second case the heat flow will be along the axis of the cylinder, that is to say essentially 1-dimensional. Accordingly, we conclude that for bulk absorption we must use D=2 and r=b, the radius of the cylinder, so that the arrival time is $b^2/4\alpha$. For surface absorption, on the other hand, we must take D=1 and r=L/2, half of the length of the cylinder, so that the arrival time for surface absorption turns out to be $L^2/8\alpha$. The ratio between the two arrival times is then $2(b/L)^2$.

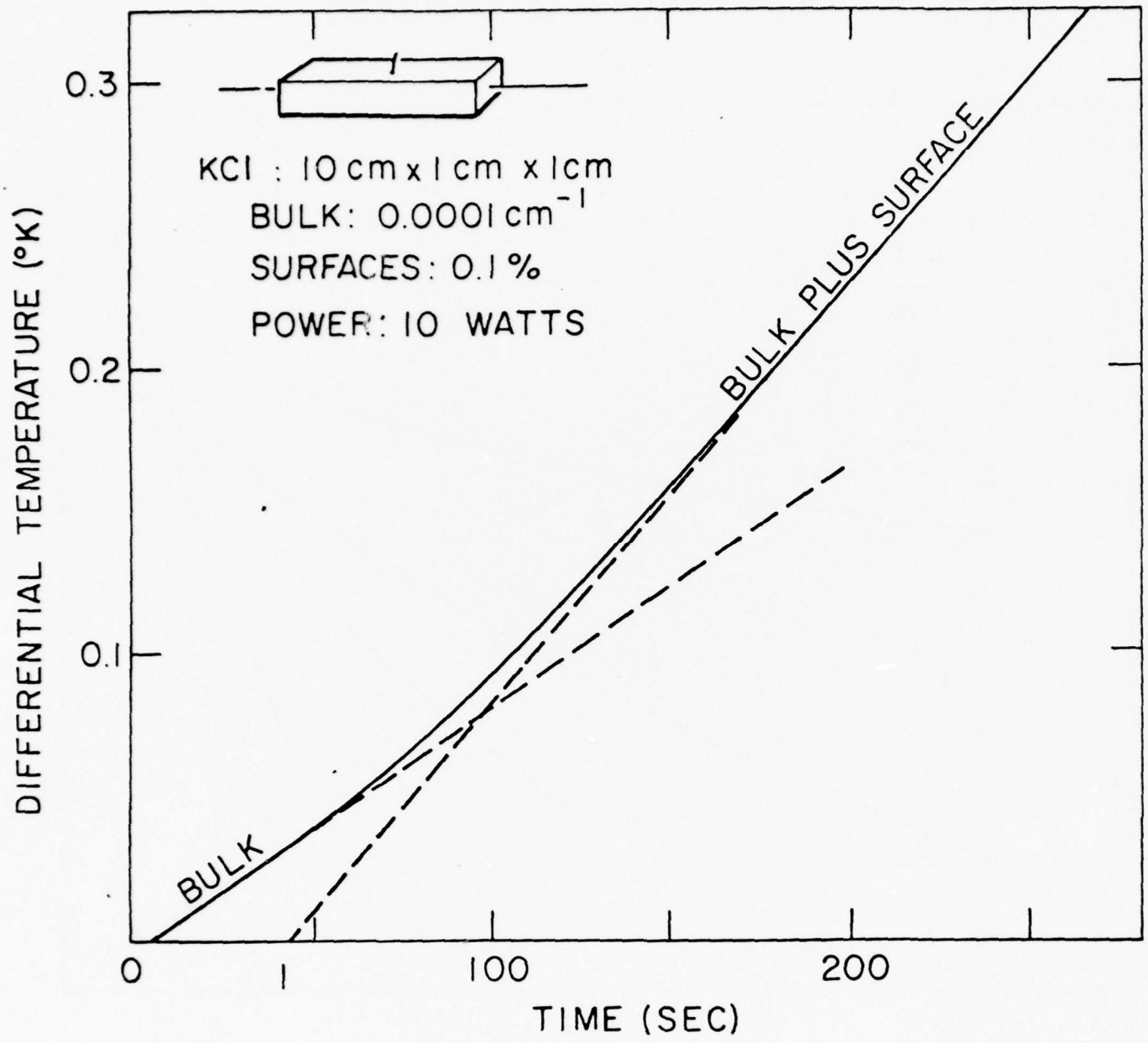
KCl : 10 cm x 1 cm x 1 cm
BULK: 0.0001 cm⁻¹
SURFACES: 0.1 %
POWER: 10 WATTS
BULK PLUS SURFACE
BULK
DIFFERENTIAL TEMPERATURE (°K)
0.3
0.2
0.1
0
1
100
200
TIME (SEC)

Fig 1

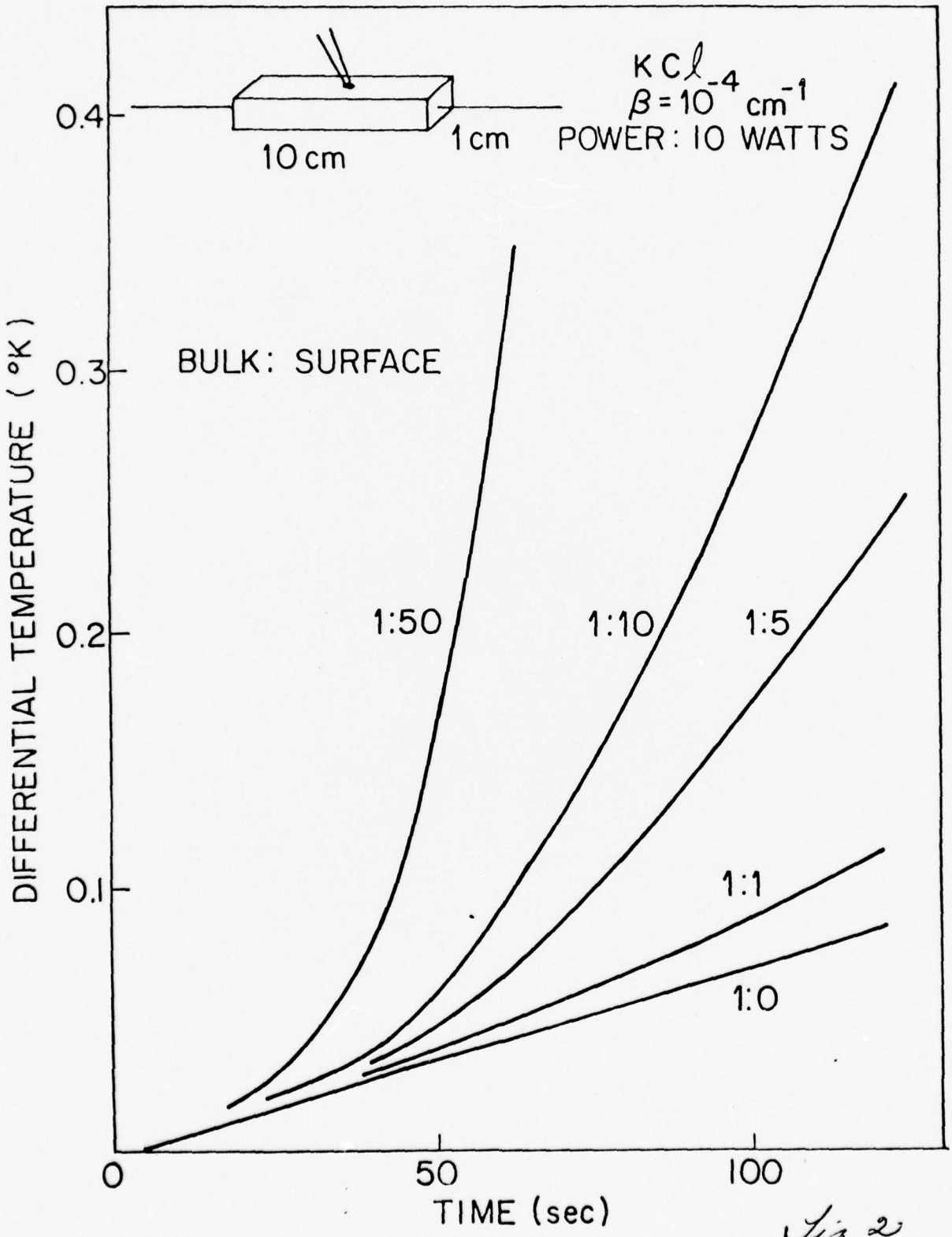
KCl
β = 10^-4 cm^-1
POWER: 10 WATTS
10 cm
1 cm
BULK: SURFACE
1:50
1:10
1:5
1:1
1:0
DIFFERENTIAL TEMPERATURE (°K)
0.4
0.3
0.2
0.1
0
50
100
TIME (sec)

Fig 2

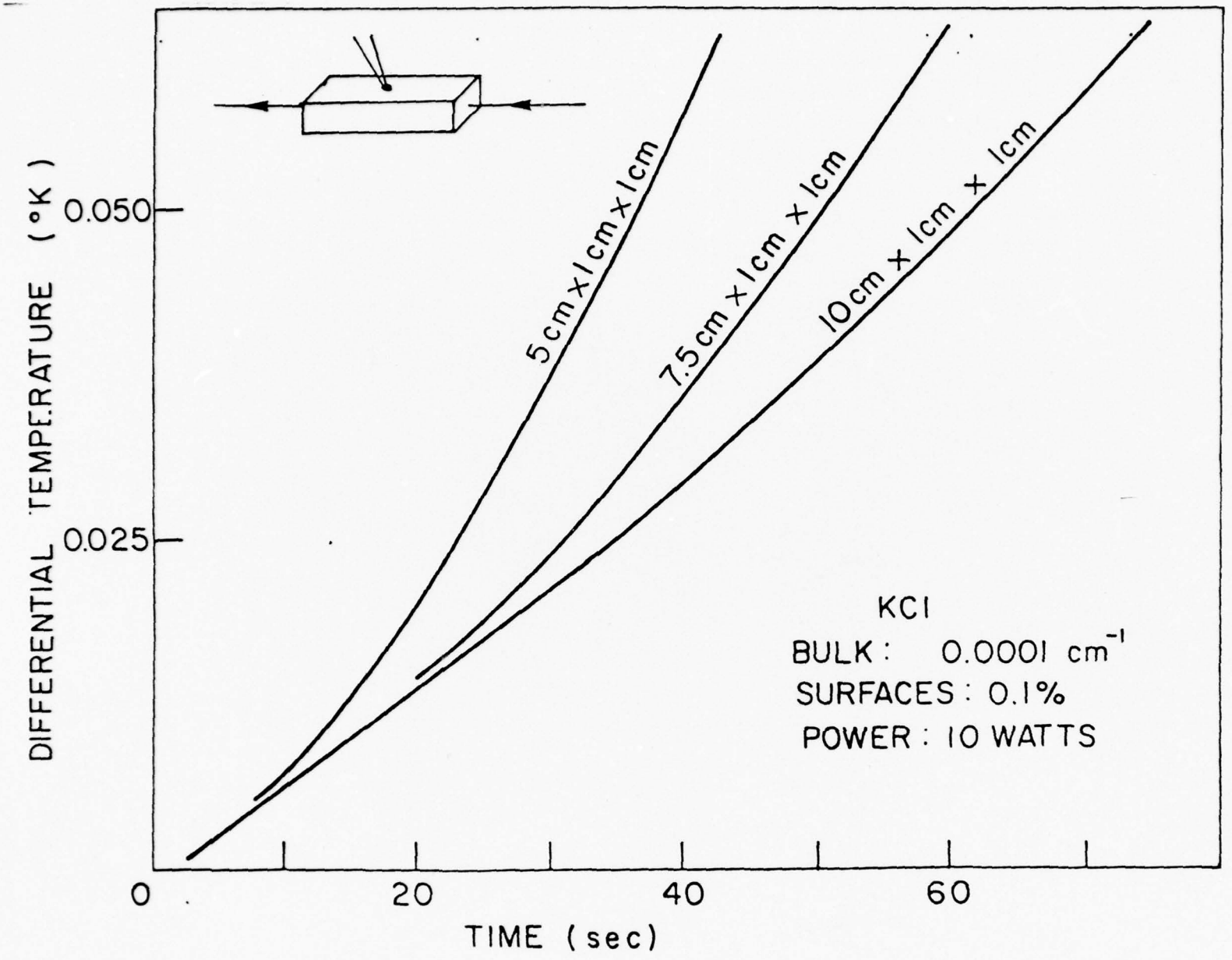
DIFFERENTIAL TEMPERATURE (°K)
0.050
0.025
0
20
40
60
TIME (sec)
5cm x 1cm x 1cm
7.5cm x 1cm x 1cm
10cm x 1cm x 1cm
KCl
BULK : 0.0001 cm⁻¹
SURFACES : 0.1%
POWER : 10 WATTS

Fig 3

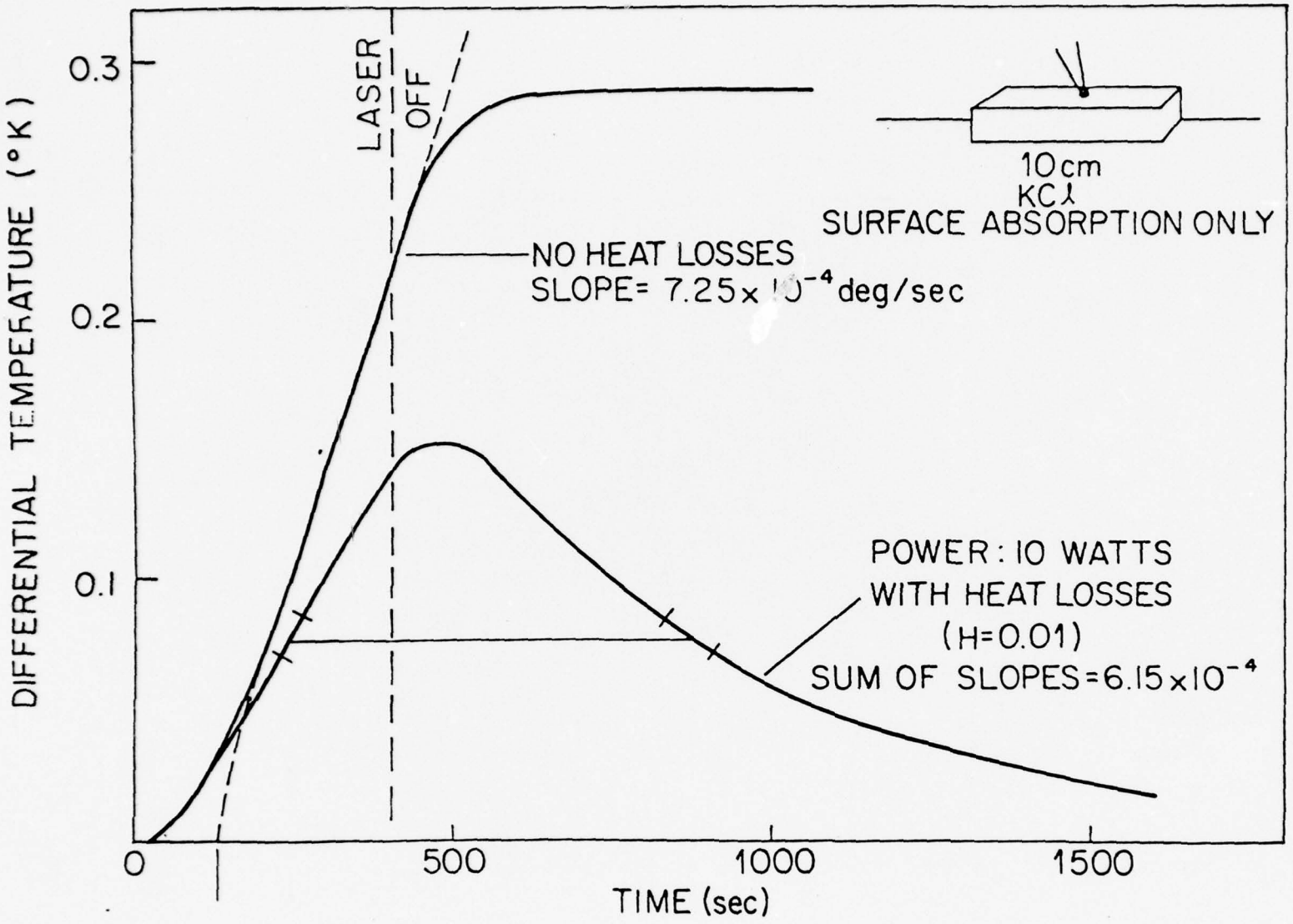
DIFFERENTIAL TEMPERATURE (°K)
0.3
0.2
0.1
0
500
1000
1500
TIME (sec)
LASER
OFF
10 cm
KCl
SURFACE ABSORPTION ONLY
NO HEAT LOSSES
SLOPE= 7.25x 10⁻⁴ deg/sec
POWER: 10 WATTS
WITH HEAT LOSSES
(H=0.01)
SUM OF SLOPES=6.15x10⁻⁴

Fig 4

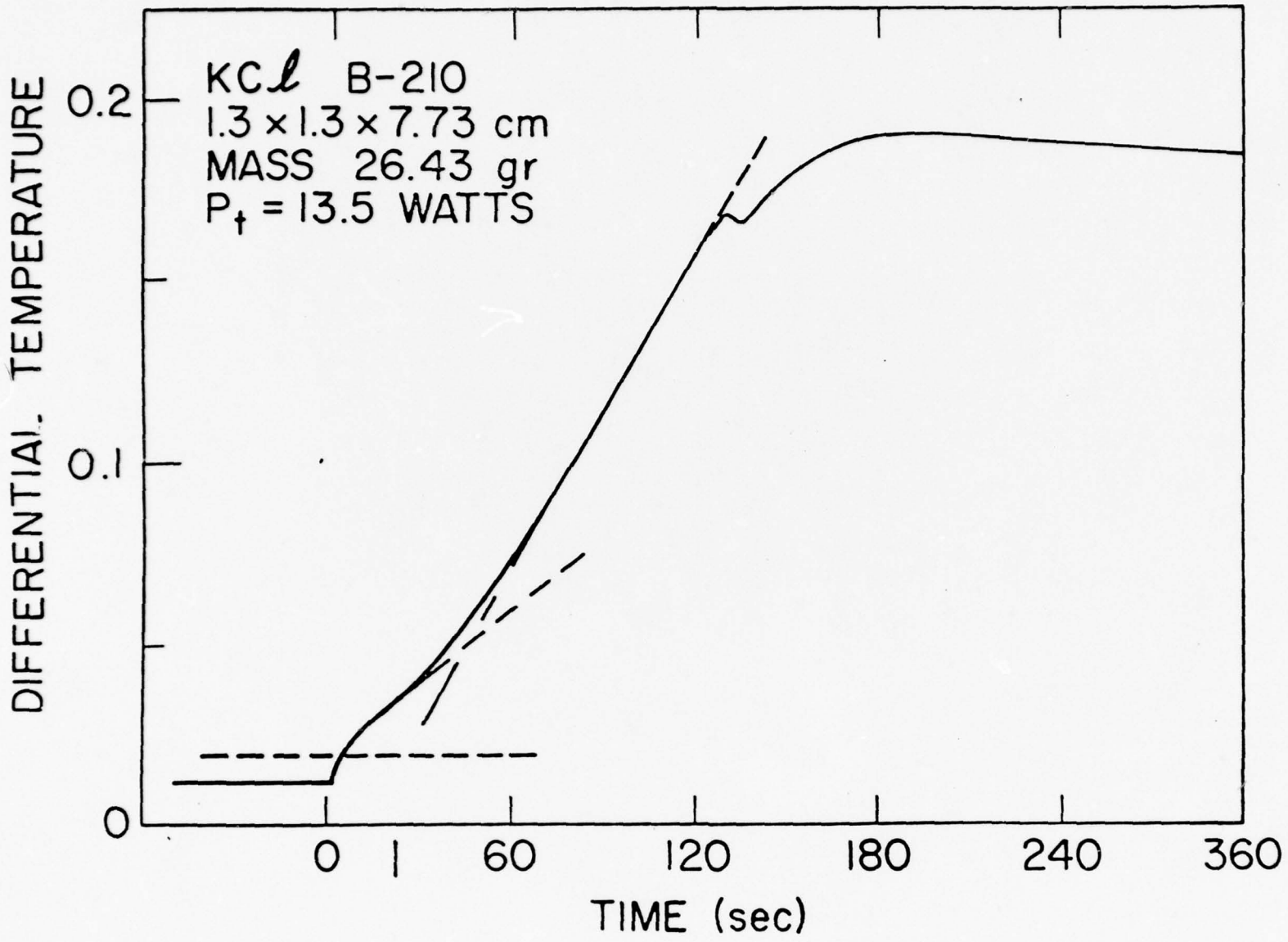
KCl B-210
1.3 x 1.3 x 7.73 cm
MASS 26.43 gr
P_t = 13.5 WATTS
DIFFERENTIAL TEMPERATURE
0.2
0.1
0
0
1
60
120
180
240
360
TIME (sec)

Fig 5

Surface and Bulk Absorption Measurements-

Two Methods of Analysis*

Don A. Gregory and James A. Harrington

University of Alabama

Huntsville, Alabama 35807

and

Herbert B. Rosenstock

Naval Research Laboratory

Washington, D. C. 20375

Classical heat flow has been employed in a previous paper[1] to determine bulk and surface absorption coefficients for long, highly transparent samples. Here we present a brief outline of this method and an older method which utilizes the slopes of the temperature-time curves directly to separate surface and bulk absorption. We then compare the results of the two methods and give possible sources of error along with suggestions as to when each method of analysis would be preferred.

*Work sponsored by the Defense Advanced Research Projects Agency and the Office of Naval Research

I. INTRODUCTION

Using classical heat flow theory to determine surface and bulk absorption coefficients is not new to laser window research, neither is analyzing the heating and cooling slopes directly; but until now a direct comparison between results obtained using the two methods has not been available. Therefore, the objective is to present the two methods briefly and to analyze the data so as to demonstrate the usefulness of each method of analysis.

Sample heating and cooling curves of actual experimental data are given along with commentaries on each. This affords a chance to compare the actual experimental curves with the computer simulated curves found throughout the literature.[2,3]

II. HEAT FLOW ANALYSIS

The problem is essentially one of heat conduction in a finite cylinder (or rectangular parallelepiped) initially at a uniform temperature, then heated from time t=o to time $t=t_1$ by a source which is constant in time. We want to find the temperature at all points and times. This solution is given in detail in reference 4 and in outline form in at least one standard textbook.[5]

Using a rectangular parallelepiped as an example, we compute the heat distribution as a function of space and time. We assume the bar is initially at the temperature of the surroundings and is heated by a known source. The differential equation governing this situation is,

$$\nabla^2 T + \frac{1}{k} g(x,y,z) = \frac{1}{\alpha} \frac{\partial T}{\partial t} \qquad (1)$$

subject to the boundary conditions

$$k\frac{\partial T}{\partial n} + hT = 0 \qquad \text{(all boundaries)}. \tag{2}$$

Where:

T = temperature measured with respect to the surroundings

x,y,z = usual cartesian coordinates

k = thermal conductivity

α = thermal diffusivity

h = heat transfer coefficient

n = the normal at any point on the surface

g(x,y,z) = the source function

The source function, g(x,y,z), in general depends on time also, but for our case we assume the laser output to be constant in time, thereby simplifying the solution. The resultant equation for T(x,y,z,t) is:

$$T(x,y,z,t) = \beta \sum_{mnp} f^{(1)}_{mnp}(x,y,z) + S \sum_{mnp} f^{(2)}_{mnp}(x,y,z,t) , \tag{3}$$

Where the f's are known (although complicated) functions of g,k,α, h, and the dimensions of the sample. The terms β and S represent bulk and surface absorption respectively.

The procedure for determining β and S is one of curve fitting. An experimentally obtained set of values for T (t) is plotted, then β and S are varied in eq. (3) until a good fit is made to the points. There is, however, one complication. The heat transfer coefficient is not usually known and must also be varied until the fit is made.

III. SLOPE ANALYSIS

Determining bulk absorption coefficients using the slopes of the heating and cooling curves has been used extensively in the past[6,7] and has been shown to give reliable data. This analysis depends on Beer's Law,

$$I = I_o e^{-\beta \ell}, \tag{4}$$

Where

I_o = Incident laser intensity

I = Intensity leaving sample

β = The absorption coefficient

ℓ = The length of the sample

Using this and accounting for infinite reflections one arrives at expressions for power absorbed and transmitted:

$$P_A = (1-R)\, P_o \left[1-e^{-\beta \ell}\right] \sum_{n=o}^{\infty} \left(Re^{-\beta \ell}\right)^n \tag{5}$$

$$P_T = (1-R)^2 \; P_o e^{-\beta \ell} \sum_{m=o}^{\infty} \left(R^2 e^{-2\beta \ell}\right)^m, \tag{6}$$

Where R is the reflection coefficient and P_o is the incident power. The infinite series converge nicely and one obtains

$$\frac{P_a}{P_t} = \frac{(1 - e^{-\beta\ell})\ (1 + Re^{-\beta\ell})}{(1 - R)\qquad e^{-\beta\ell}} \tag{7}$$

The power transmitted is measured directly during the experiment and the power absorbed may be written as:

$$P_a = MC\ \frac{\Delta T}{\Delta t}\ , \tag{8}$$

Where M is the mass of the sample, C the specific heat, and $\Delta T/\Delta t$ the slope of the heating curve. The last term may be expanded using the method of Hass[8] to account for heat losses to the environment. The result is:

$$\frac{\Delta T}{\Delta t}(\text{corrected}) = \left[T_2' - T_1' - \left(T_3' - T_1'\right) \cdot \left(\frac{T_2 - T_1}{T_3 - T_1}\right)\right] . \tag{9}$$

The terms T_1, T_2, and T_3 are the temperatures of the sample at different times during the experiment; before, during, and after laser irradiation. The T' terms denote slopes of the curve during the same intervals.

Solving the previous equations for β, one obtains,

$$\beta = \frac{1}{\ell} \ln \frac{Q + \sqrt{Q^2 + 4R}}{2}, \qquad (10)$$

Where

$$Q = (1-R)\left\{\frac{MC}{P_T}\left[T_2' - T_1' - \left(T_3' - T_1'\right)\left(\frac{T_2 - T_1}{T_3 - T_1}\right)\right] + 1\right\}. \qquad (11)$$

Application of these equations to a long bar sample has been done and a sample of actual data is given in figure (1). The change in slope in region II is the important facet. It has been shown elsewhere that the initial heat rise is due to bulk absorption while the final heat rise is due to bulk and surface absorption.[2] Applying Eq. (10) then to the two heating slopes allows a separation of bulk and surface absorption coefficients.

IV. EXPERIMENTAL PROCEDURES

Methods for obtaining the temperature-time curves are discussed elsewhere in greater detail[2] and only outlined here. A vacuum calorimeter with CaF_2 windows encloses the sample which is held in place by sharpened nylon screws. The thermocouple is attached to the sample using a high thermal conductivity grease and a spring loaded, sharpened nylon rod, or glued directly to the sample with thermocouple cement.

Careful alignment of the sample in the laser beam is necessary to minimize laser light scattered directly into the thermocouple. This is accomplished by positioning a small HeNe laser so that the visible laser light is coaxial with the invisible HF/DF beam. One can then adjust the position of the sample until the reflections from both polished surfaces lie along the same line. The HF/DF laser is then turned on and the temperature time curve obtained via a Keithley nanovoltmeter and an Omniscribe strip chart recorder.

V. COMPARISON OF RESULTS

In table 1 values of the absorption coefficients obtained by the two methods of analysis are given and a discussion of error follows. Agreement is generally good for the bulk absorption coefficient and poor for the surface absorption. This result is as yet inexplicable unless one postulates the initial method for obtaining the surface absorption using the slope analysis method, ie:

$$\ell \left[\beta \text{ (bulk + surface)} - \beta \text{ (bulk)}\right] = \beta \text{ (surface)} \qquad (12)$$

is in error. This is indeed possible since the previous equation is phenomenological in derivation.

VI: ERROR CONSIDERATIONS

A. Slope Analysis

Two major sources of error have been observed using the slope analysis method: air currents inside an open air calorimeter and inaccuracies in evaluating the two heating slopes.

Fluxuating environmental temperature during the course of a measurement has been controlled by making two improvements: a vacuum calorimeter and an ice point thermocouple reference. The vacuum calorimeter eliminated the flow of air currents around the sample and also made the determination of the heat transfer coefficient more accurate. In the past a noticeable change in this coefficient during a measurement has been observed, which tends to make the curve fitting more difficult and less accurate.

Originally a room temperature reference composed of a block of aluminum enclosed in an insulating material was used. This was found unsatisfactory when it was discovered that the room temperature could change as much as $10^{\circ}F$ during a working day. To combat this, an ice water reference was employed and proved to be quite stable over the course of a measurement.

The separation of surface and bulk absorption using this method depends solely on the change in the heating slope during irradiation of the sample. Two sample curves are given in Fig. (1) and Fig. (2). If the bulk absorption is much larger than the surface absorption, the change in slope may be only slightly detectable thus making the distinction between surface and bulk absorption almost impossible using this method.

Other smaller sources of error have been noted. They are: thermocouple attachment to sample, nanovoltmeter instability, laser output stability and beam divergence. Through practice these problems have been characterized and reduced to the point of no longer being major sources of error.

B. Heat Flow Analysis

This method depends heavily on the experimentally obtained temperature - time curve, thus all errors of the previous section are still present when the curve fitting is done. Often several different parameters can be constructed so as to fit the experimental curve. This is a great source of miscontent when doing the curve fitting, which can only be overcome by doing many possible fits, then choosing the best. If the experimentally derived curve was in error due to some of the previously mentioned sources, the curve fitting could possibly still give a reasonable fit to the inaccurate data, thereby reinforcing the data obtained experimentally.

With these thoughts in mind, one can see that the major source of error using this method still lies with the experimental arrangement. If the experiment is done carefully however, much more information can be obtained using this method. The temperature at all points and times can be known thus making the determination of surface and bulk absorption easier and more reliable since it does not rely as heavily on personal judgement which can add substantially to the total error of the measurement.

VII. CONCLUSIONS

In this paper we have presented two methods of determining surface and bulk absorption of a long bar sample and given results obtained using both methods. Each method has its advantages. The temperature rise method is relatively quick, simple and accurate if certain criteria mentioned in the error discussion are met. The heat flow method can only be as accurate as the experimental curve, but more information can be gained if the experiment has been done carefully. We must conclude therefore that neither method should be used for all absorption studies, but rather each should be considered in light of the sample being characterized.

REFERENCES

1. H. B. Rosenstock, D. A. Gregory, and J. A. Harrington, Applied Optics, Vol. 15, No. 9, Sept. 1976.
2. M. Hass, J. W. Davisson, H. B. Rosenstock and J. Babiskin, Applied Optics, Vol. 14, No. 5, May 1975.
3. H. B. Rosenstock, M. Hass, D. A. Gregory, and J. A. Harrington, to be published, Applied Optics.
4. H. B. Rosenstock in "High Energy Laser Windows", Semiannual Report 6 on ARPA Order 2031, Naval Research Laboratory, Washington, D. C., 30 Sept. 1975.
5. N. Ozisik, Boundary Valve Problems of Heat Conduction (International Textbook Co., Scranton, PA., 1968).
6. J. A. Harrington, D. A. Gregory and W. F. Otto, Jr., Applied Optics, Vol. 15, No. 8, August, 1976.
7. J. Rowe and J. A. Harrington, J. Applied Physics, Vol. 47, No. 11, Nov. 1976.
8. M. Hass, J. W. Davisson, P. H. Klein, and L. L. Boyer, J. Applied Physics, Vol. 45, No. 9, Sept. 1974.

CAPTION

Fig. 1 Experimentally obtained temperature vs. time plot for a long bar sample at 10.6 μm.

FIG. 1

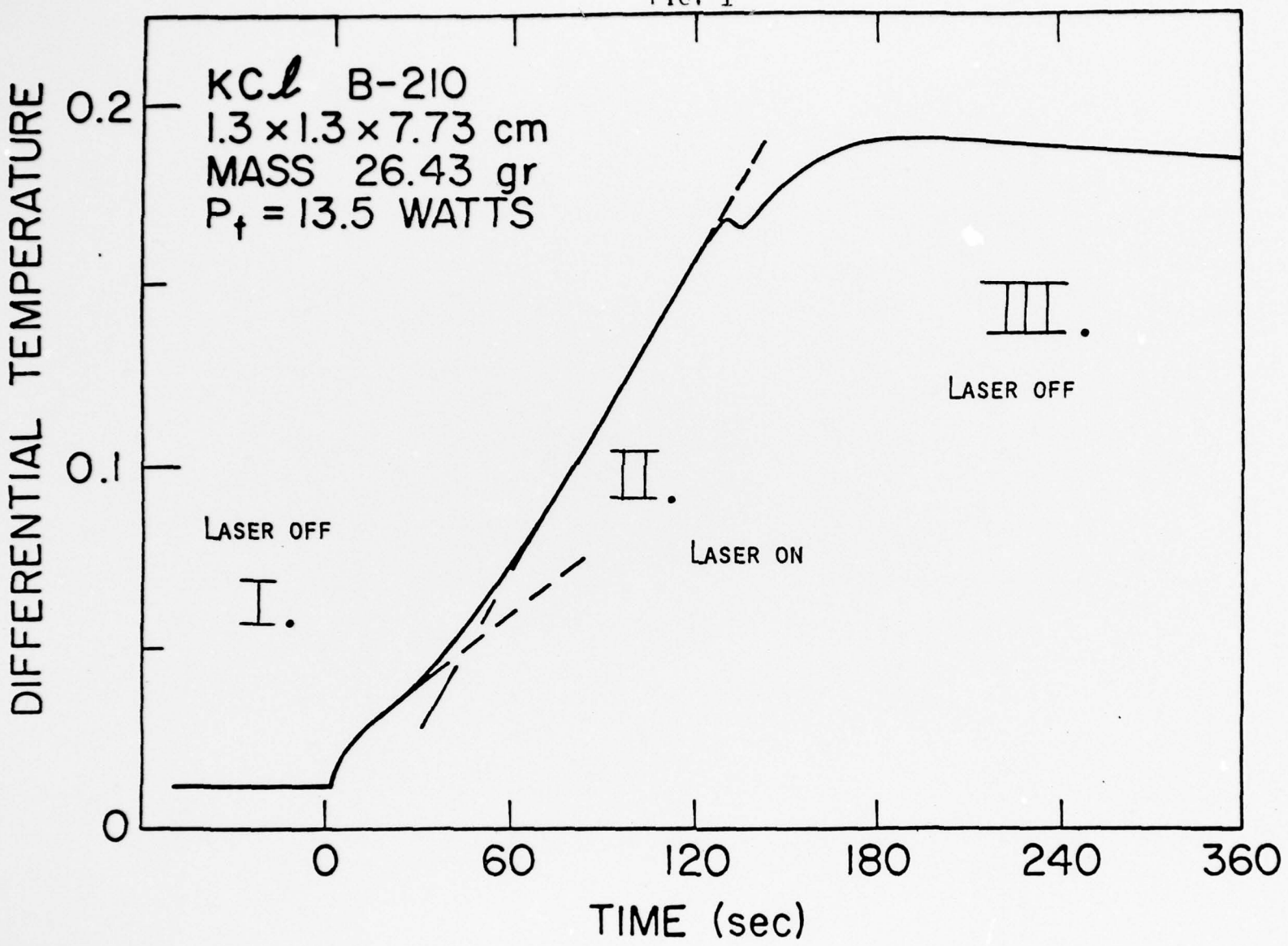
KCl B-210
1.3 × 1.3 × 7.73 cm
MASS 26.43 gr
P_t = 13.5 WATTS
DIFFERENTIAL TEMPERATURE
0.2
0.1
0
I.
LASER OFF
II.
LASER ON
III.
LASER OFF
0
60
120
180
240
360
TIME (sec)

CAPTION

Table 1 A comparison of data obtained using the two methods of analysis.

Table 1

	Heat Flow Analysis		Slope Analysis	
	Bulk Absorption Coefficient (cm^{-1}) $X10^{-4}$	Fractional Power absorbed at surfaces $X10^{-4}$	Bulk Absorption Coefficient (cm^{-1}) $X10^{-4}$	Fractional Power absorbed at surfaces $X10^{-4}$
		2.7 Microns		
KBr	.50	3.1	1.2	8.5
Znse	14	3.2	9.8	13
CaF_2	1.7	4.7	1.7	18
NaF:LiF	7.9	4.1	8.8	16
		3.8 Microns		
Znse	11	4.4	11	17
CaF_2	2.5	3.6	2.8	6.5
Nacl	9.0	400	5.9	90

CONCLUSIONS

In this report we have described new materials for possible use as laser windows. We have only looked at a few of the possibilities in the new materials area; there are many others to be investigated and the materials we have looked at merit further investigation since some of the materials are relatively new and methods of fabrication most certainly will improve.

The method of long bar calorimetry is relatively new and should be explored further, especially in the experimental area where reliable data is rare. It is our belief that this method, although it does have limitations, contains a wealth of information if we are just able to discern it.